Journal of Integrative Agriculture 2026, 25(9): 3572–3584

Available online at ScienceDirect

Journal of Integrative Agriculture

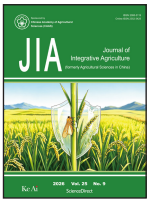

RESEARCH ARTICLE

Genome-wide characterization of soybean lysophosphatidic acid acyltransferases and functional characterization of the role of *GmLPAT11* in salt stress

Zhiyang Wang*, Peiyan Liu*, Haitong Sun, Wenying Suo, Ziqian Cheng, Mingliang Yang#, Qingshan Chen#, Ying Zhao#

National Key Laboratory of Smart Farm Technology and Systems/Key Laboratory of Soybean Biology, Ministry of Education/Northeast Agricultural University, Harbin 150030, China

Highlights

- Under salt stress, *GmLPAT11* enhances soybean salt tolerance by regulating antioxidant activity and redox status.
- Two haplotypes of the *GmLPAT11* gene were identified. The natural variation of *GmLPAT11* is crucial for its function, with Hap2 being a favorable haplotype for salt tolerance.

Abstract

Lysophosphatidic acid acyltransferase (LPAT) enzymes are widely expressed in various plant species, and they contribute to growth, development, and stress responses. Currently, information regarding the *LPAT* gene family in soybeans is limited. In this study, genome-wide analyses identified 15 soybean *LPATs*, which were then evaluated for their conserved protein motifs. These genes were grouped into three clusters based on their phylogenetic relationships. Confocal microscopy was used to visualize the localization of six *GmLPATs* within *Arabidopsis* mesophyll protoplasts. *cis*-Acting regulatory element analyses and qRT-PCR experiments revealed that these *GmLPATs* were upregulated in response to hormonal stimulation or exposure to abiotic stressors, including drought, alkaline conditions, and salt stress. The expression patterns of these *GmLPATs* varied among different soybean tissue types. One member of the solLPAT1 subtype (*GmLPAT11*) was found to be upregulated in response to a range of treatments, highlighting its role in soybean salt stress responses. *GmLPAT11* expression in *Escherichia coli* confirmed the LPAT activity of this recombinant enzyme, and overexpressing this LPAT reduced reactive oxygen species production in transgenic soybean plants, thereby enhancing their salt stress tolerance. Gene association analyses indicated that *GmLPAT11* variants are closely associated with seedling salt tolerance, and a polymorphism in the *GmLPAT11* CDS region was potentially associated with salt tolerance. These results provide new insights into the nature of the *LPAT* gene family in soybeans while also identifying promising candidate genes for future research efforts to enhance the overall salt tolerance of soybean crops.

Keywords: soybean (*Glycine max* (L.) Merr.), lysophosphatidic acid acyltransferase, salt stress, expression pattern

1. Introduction

Phosphatidic acid (PA) functions as a signaling molecule in plants, and it mediates various physiological processes including the osmotic stress response (Wang *et al.* 2006; Hong *et al.* 2016). Lysophosphatidic acid acyltransferases (LPATs) are essential enzymes in the Kennedy pathway that catalytically process fatty acid chains to synthesize 3-phosphoglycerate and facilitate triacylglycerol oil production (Misra *et al.* 2014). LPATs are widely distributed among various animal, plant, and microbial species, and their broad substrate specificity is important for establishing overall lipid acyl composition (Snyder *et al.* 2009).

Received 20 September 2024; Received in revised form 20 November 2024; Accepted 25 November 2024; Available online 28 December 2024
Zhiyang Wang, E-mail: wzy13613642168@163.com; Peiyan Liu, E-mail: liupeiyan823@163.com; #Correspondence Mingliang Yang, Tel: +86-451-55191945, E-mail: mlyang@neau.edu.cn; Qingshan Chen, Tel: +86-451-55191259, E-mail: qshchen@126.com; Ying Zhao, E-mail: tianshi198937@126.com

* These authors contributed equally to this study.

doi: 10.1016/j.jia.2024.12.031

To date, members of the *LPAT* family have been characterized in *Arabidopsis thaliana* (Kim *et al.* 2005), *Oryza sativa* (Shaikh *et al.* 2022), *Zea mays* (Brown *et al.* 1994), *Arachis hypogaea* (Chen *et al.* 2012), *Cocos nucifera* (Knutzon *et al.* 1995), *Brassica napus* (Bourgis *et al.* 1999), *Ricinus communis* (Arroyo-Caro *et al.* 2013), and *Tropaeolum majus* (Taylor *et al.* 2010), with a majority serving as key regulators of oil synthesis and stress responses in their respective plant species. Seven putative LPAT isoforms are encoded in the *Arabidopsis* genome. Their evolutionary associations, substrate preferences, and subcellular localization patterns can be used to categorize them into plastid-localized LPAT1 with a substrate preference for 16:0 over 18:1 CoA (Kim and Huang 2004), endoplasmic reticulum (ER)-localized LPAT2-LPAT5 with an 18:1 CoA substrate preference (Ohlrogge and Browse 1995), and soluble LPAT (solLPAT1), which acylates LPA to produce PA (Misra *et al.* 2014). The different LPAT subtypes likely fulfill distinct functional roles, as evidenced by their varied expression patterns and activities. In *Arabidopsis*, there is only one gene encoding the form in plastids, *AtLPAT1*. Mutation or deletion of *AtLPAT1* can lead to embryonic death. This gene strongly prefers 18:1-CoA over 16:0-CoA (Ohlrogge and Browse 1995). Cytoplasmic *LPAT* genes have been reported in the mature seeds or organs of species such as *Z. mays* (Brown *et al.* 1994), *C. nucifera* (Knutzon *et al.* 1995), and *Limnanthes alba* (Hanke *et al.* 1995). Transgenic *Arabidopsis* seeds overexpressing homologous rapeseed *LPAT2* show increased TAG content and quality (Maisonneuve *et al.* 2010). *TmLPAT2* and *EpLPAT2* are key TAG assembly regulators (Taylor *et al.* 2010). The *Arabidopsis AtLPAT4* and *AtLPAT5* genes also generate alternative transcripts that may be associated with greater PA complexity (Chapman and Ohlrogge 2012). However, few reports to date have focused on other members of the *LPAT* gene family.

Plants encounter various abiotic stressors during their growth and development, including drought, temperature extremes, salinity, ion toxicity, and mineral deficiencies, all of which can have adverse effects through reductions in the rates of photosynthesis and respiration related to cell membrane damage. These abiotic stressors can also regulate *LPAT* expression, and some studies have specifically evaluated the effects of drought, high salt, cold exposure, auxin analogs, and osmotic pressure on *LPAT* levels. Cold stress can suppress *Arabidopsis* LPAT1 expression, leading to a decline in the abundance of phosphatidylglycerol-containing fatty acids with a high melting point and thereby helping plants adapt to growth under cold conditions (Kim *et al.* 2010). In the roots of *Arabidopsis*, LPAT2 is involved in stimulating glyceride biosynthesis, which allows these plants to more effectively respond to phosphate starvation (Angkawijaya *et al.* 2017). PLD-derived PA has been studied extensively and shown to be involved in plant responses to drought and salt stress (Zhang *et al.* 2004, 2012; Mishra *et al.* 2006; Bargmann *et al.* 2008; Hong *et al.* 2008; Wang *et al.* 2019; Ali *et al.* 2022). In rice, the PA generated by LPAT2 has also been shown to play a positive role in controlling tolerance to osmotic stress conditions (Shaikh *et al.* 2022).

Studies identifying multiple *LPATs* across plant species and employing transgenic approaches have demonstrated the functional significance of these genes. However, no studies to date have comprehensively characterized the soybean *LPAT* gene family. Thus, any efforts to fully analyze these genes can potentially provide new insights into the structural and functional features of this crop species, aiding in crop improvement efforts (Zhou *et al.* 2025). Soybean plants generally grow in light soil but have limited tolerance for saline or alkaline conditions. Salinity adversely affects soybean growth, agronomic traits, and seed quality, significantly reducing yield and sometimes resulting in crop failure. Identifying the genes associated with saline–alkali tolerance and clarifying their molecular mechanisms are essential for developing soybean varieties adapted to saline soil. In this study, bioinformatics techniques were employed to identify 15 soybean *LPAT* genes and analyze their phylogeny, gene structures, protein structures, *cis*-regulatory elements, and expression patterns in response to abiotic stressors. NaCl treatment upregulated *GmLPAT11* expression, suggesting its role in soybean responses to salt stress. Enzyme kinetics experiments further showed that purified GmLPAT11 could convert C18:1 CoA into PA. Overexpression of *GmLPAT11* in soybean hairy roots improved salt tolerance, increased antioxidant enzyme activities, and reduced cellular redox status. A natural soybean population was analyzed to assess the *GmLPAT11* variations associated with salt tolerance, which facilitated the identification of salt-tolerant GmLPAT11 alleles *via* haplotype analysis. Together, the results of this study highlight the potential of *GmLPAT11* as a candidate gene for future efforts to improve soybean salt tolerance.

2. Materials and methods

2.1. Soybean *LPAT* gene identification

The whole genome and protein sequences of soybean were retrieved from the Phytozome v12.1 database (https://phytozome.jgi.doe.gov/pz/portal.html). LPAT protein sequences from *A. thaliana* (Arabidopsis Information Resource (TAIR); https://www.arabidopsis.org/) were used for BLASTP queries of the soybean genome with an e–value cutoff of 1.0. Each candidate gene was confirmed as encoding the LPAT enzyme (EC:2.3.1.51) using Phytozome, and redundant sequences were removed manually. The subcellular localization of each LPAT protein in soybean was predicted using WoLF PSORT (https://www.genscript.com/wolf-psort.html), and the molecular weight, isoelectric point, and sequence length were calculated using ExPASy (https://cn.expasy.org/tools).

2.2. Evolution, genetic structure, and synteny analyses

A phylogenetic tree was constructed in MEGA 5.0 using homologous *LPAT* gene sequences from *Glycine max* (*GmLPAT*), *A. thaliana* (*AtLPAT*), *Phaseolus vulgaris* (*PvLPAT*), *Z. mays* (*ZmLPAT*), and *O. sativa* (*OsLPAT*) (Tambasco-Studart *et al.* 2005). The gene information is shown in Appendix A. Protein sequences were aligned with ClustalW to identify conserved domains. Gene exon–intron structures were visualized using Gene Structure Display Server v2.0 (https://gsds.gao-lab.org). Synteny among the

LPATs from different plant species was assessed with the PGDD database (https://chibba.agtec.uga.edu/duplication/).

2.3. *GmLPAT* promoter analyses

cis-Regulatory elements were scanned in the 2 kb upstream putative promoter regions of each *GmLPAT* gene using the PlantCARE database (https://bioinformatics.psb.ugent.be/webtools/plantcare/html/) (Liu *et al.* 2015).

2.4. Analyses of *GmLPAT* expression

GmLPAT transcriptional profiles in leaves, flowers, seeds, pods, and roots were analyzed using high-throughput sequencing data from the Phytozome database, with the results shown in hierarchically clustered heatmaps (Chen *et al.* 2020). The transcriptional responses of these *GmLPATs* to hormonal stimulation and abiotic stress were assessed by transplanting soybean seedlings at the second trifoliolate stage into solutions containing 100 mmol L^{-1} $NaHCO_3$, 200 mmol L^{-1} mannitol, 150 mmol L^{-1} NaCl, 20% PEG6000, 100 μmol L^{-1} jasmonic acid (JA), 100 μmol L^{-1} salicylic acid (SA), 100 μmol L^{-1} abscisic acid (ABA), or 100 μmol L^{-1} brassinolide (BR). At 0, 1, 3, 6, 12, and 24 h after transplantation, root samples were snap-frozen in liquid nitrogen and stored at –80°C.

RNA was extracted from these samples using a Quick Total RNA Isolation Kit (Huayueyang, Beijing, China). RNA concentration and quality were assessed, and integrity was confirmed by 1% agarose gel electrophoresis. First-strand cDNA was prepared using Prime Script® RT Master Mix (TaKaRa, Dalian, China) and diluted to 500 ng L^{-1}. qPCR was conducted with SYBR Green (TaKaRa) on a Roche LightCycler® 96 System following the manufacturer's protocol (Bustin *et al.* 2009). The 20 μL qPCR reactions included 10 μL of 2× real-time PCR Mix, 0.5 μL of each primer, and cDNA in an appropriate volume. Thermocycler settings consisted of 95°C for 30 s; 35 cycles of 95°C for 10 s, 60°C for 30 s, and 95°C for 15 s; and then a final incubation at 60°C for 60 s and 95°C for 15 s. *GmLPAT* transcript levels were normalized to root mRNA levels under basal conditions, with *GmGAPDH* (Genbank no.: DQ355800) and *GmACTIN* (Genbank no.: AF049106) serving as reference genes (Zhao *et al.* 2021). Gene expression was quantified using the $2^{-\Delta\Delta Ct}$ method. The primers used for these analyses are given in Appendix B.

2.5. Analyses of subcellular localization

The complete coding regions of *GmLPAT* genes were amplified from root samples of the 'DN50' soybean cultivar. These genes were then introduced to the GFP-encoding pBI121 vector to create GmLPATs::GFP fusion proteins and cloned using gene-specific primers (Appendix B). After PEG-calcium-mediated co-transformation and a 16 h incubation, recombinant GmLPAT::GFP plasmids were transiently expressed in *Arabidopsis* mesophyll protoplasts (Yoo *et al.* 2007). The empty vector served as a positive control, and Mito-Tracker Red CMXRos (Beyotime, C1049B, China) was used as a mitochondrial marker (Chen J *et al.* 2022; Chen X *et al.* 2022). The localization of these GFP-labeled proteins within cells was assessed using confocal laser-scanning microscopy (Carl Zeiss LSM710, Germany).

2.6. Enzyme kinetic analyses

LPAT activity levels were analyzed using *E. coli* membrane extracts as described previously (Tóth *et al.* 2016), and relied on the reaction between CoA and Ellman's reagent DTNB. Optimized reactions were conducted in a 400 μL volume containing 100 mmol L^{-1} phosphate buffer (pH 7.5), 120 μmol L^{-1} DTNB, 50 μmol L^{-1} 18:1-LPA or 18:1-OH-LPA, either 2 mmol L^{-1} EDTA (minus Mg^{2+} assays) or 1 mmol L^{-1} $MgCl_2$, 20–40 μmol L^{-1} of different acyl-CoAs, and 30–320 μg of membrane extract protein. After 30 s of pre-incubation with the extract, acyl-CoA was added, and the absorbance at 410 nm was measured for 3 min. Released CoA was quantified using the molar absorption coefficient of ε=13,600 M^{-1} cm^{-1}. Initial reaction slopes were used to calculate enzymatic activity, expressed in nanomoles of CoA released per min.

2.7. *GmLPAT11* overexpression in soybean hairy roots

The pSOY1-*GmLPAT11* overexpression vector was constructed by cloning the *GmLPAT11* coding sequence into pSOY1, which contains the CaMV35S promoter, using primers listed in Appendix B. The pSOY1-*GmLPAT11* recombination plasmid was electroporated into *Agrobacterium rhizogenes* strain K599 for soybean hypocotyl transformation. The transformation of DN50 hypocotyls and induction of hairy roots were performed as described previously (Tóth *et al.* 2016), with hairy roots from K599-infected soybeans serving as controls. PCR and enzyme activity assays were used to confirm transgenic hairy roots, with non-transgenic lines removed from the sample population. The impact of transgenic hairy roots on various physical and biochemical parameters was assessed using 10–20 transgenic hairy roots. These roots were exposed to either 0 or 120 mmol L^{-1} NaCl for 5 d, after which the maximum root length, fresh root weight, leaf fresh weight, and plant height were measured.

2.8. Biochemical and physiological analyses

After 3 d of stress treatment, root length and plant height were measured for 10 plants per group. Roots were separated from shoots, blanched for 15 min at 105°C, dried to a constant weight at 80°C, and then weighed to determine the aboveground and belowground dry weights. The leaves of 10 seedlings were rinsed with distilled water, blotted dry, and weighed to determine fresh weight.

Spectrophotometry was used to measure hydrogen peroxide (H_2O_2) and superoxide ($O_2^{-}\cdot$) levels (Velikova *et al.* 2000; Fryer *et al.* 2002). Soybean extracts (0.5 g) were prepared in a 15 mL solution containing 0.5 mmol L^{-1} ascorbic acid (ASA), 1% (w/v) PVP, 1.5 mmol L^{-1} EDTA, and 50 mmol L^{-1} K_2HPO_4-KH_2PO_4 (pH 7.04). Peroxidase (POD), superoxide dismutase (SOD), and ascorbate peroxidase (APX) antioxidant activity levels were then measured in the supernatant from this solution (Giannopolitis and Ries 1977; Nakano and Asada 1981).

Leaves from WT and overexpressing plants were stained after either 0 or 2 h of stress treatment by immersion in 1.5 mL of NBT, DAB, or Evan's blue staining solutions at room temperature overnight. The leaves were then destained in a

boiling water bath containing 75% ethanol and 5% glycerol.

Propidium iodide (PI) staining of WT and overexpressing root tips was performed after 12 h of stress treatment by immersing roots in a 20 μg mL^{-1} PI solution for 30 min, followed by three washes with distilled water before imaging with a laser confocal microscope. The CoroNa™ Green Sodium Indicator staining of WT and overexpressing root tips was conducted after 12 h of stress treatment by immersing roots in CoroNa™ Green solution for 30 min, followed by three rinses with distilled water before imaging with a laser confocal microscope.

2.9. Haplotype analyses

Haplotype analysis of *GmLPAT11* was conducted using 547 genetically diverse Chinese germplasm resources with varying salt tolerance index (STI) values. The 547 varieties included 365 varieties and 182 local varieties, 93.60% of which were from Northeast China (Heilongjiang, Liaoning, Jilin, and Inner Mongolia). They included 363 cultivars and 149 landraces from Northeast China; two cultivars and two landraces from Northwest China; 30 landraces from North America; and one cultivar from Japan. After 5 d of exposure to salt stress (120 mmol L^{-1} NaCl), the plant height, root length, aboveground fresh weight, and belowground fresh weight were measured. Principal component and membership function analyses were then conducted, and a comprehensive index and STI values were calculated (Han *et al.* 2006; Dai *et al.* 2014; Zhang *et al.* 2021). Candidate gene sequences were obtained from Phytozome, and local BLAST analysis was performed using *GmLPAT11* sequence data and unpublished genomic data from the resequencing of the 547 germplasm resources, enabling single nucleotide polymorphism (SNP) identification and analysis. *GmLPAT11* SNP haplotype distributions in the germplasm populations were analyzed with DnaSP 5.0 (Librado and Rozas 2009), excluding haplotypes with frequencies below 5% among the cultivars. The significance of phenotypic variation among haplotypes was analyzed in SPSS using ANOVA with Duncan's multiple range test.

3. Results

3.1. Soybean LPAT identification

A search of the soybean genome identified 15 *LPAT* genes, tentatively named *GmLPAT1*-*GmLPAT15* (Table 1). The proteins encoded by these genes ranged in length from 248 to 457 amino acids, with molecular weights from 28.06 to 50.50 kDa and isoelectric points from 5.127 to 10.231.

Comparative phylogenetic analyses of LPATs encoded in the soybean, *Arabidopsis*, rice, maize, and common bean genomes classified these LPATs into three groups: LPAT1, LPAT2, and solLPAT1 (Fig. 1-A). The LPAT1 (*GmLPAT5* and *GmLPAT9*) and LPAT2 (*GmLPAT6*, *GmLPAT7*, *GmLPAT8*, *GmLPAT10*, *GmLPAT12*, *GmLPAT13*, and *GmLPAT15*) proteins were closely related, while solLPAT1 (*GmLPAT3*, *GmLPAT4*, *GmLPAT11*, and *GmLPAT14*) proteins formed a distinct clade, consistent with previous studies.

To further explore the relationships between gene evolution and the proteins they encode (Kolkman and Stemmer 2001; Liu *et al.* 2005), the domain organization and exon–intron structures of these *GmLPATs* were analyzed (Fig. 1-C). Acyltransferase and abhydrolase domains were shared by the LPAT1, LPAT2, and solLPAT1 proteins. Exon–intron organization analyses indicated that the structural evolution of these proteins involved highly similar exon numbers and positions within each family. The sequence alignment of *LPATs* from various plant species revealed two highly conserved regions, each with consensus motifs: Motif I, $NH(X)_4D$; Motif II, EGT (Taylor *et al.* 2010; Sivakumar and Sivaraman 2011). These residues are highly conserved among acyltransferases and play an essential role in catalyzing fatty acid transfer from acyl-CoA to G3P analogs (Lewin *et al.* 1999). No previous comparative studies have detailed the conserved residues or distinct motifs differentiating proteins in the LPAT1, LPAT2, and solLPAT1 subfamilies in soybean.

3.2. *GmLPAT* synteny and gene structure analyses

LPAT genes in the soybean, *Arabidopsis*, rice, maize, and

Table 1 Basic information on the 15 soybean *LPAT* genes (*GmLPATs*)

Gene name	Gene ID[1)]	Gene location	Protein length (aa)	Isoelectric point	Molecular weight (kDa)
GmLPAT1	Glyma.02G181300	Gm2 32801499–32809390	385	9.621	43.24
GmLPAT2	Glyma.03G139700	Gm3 36761439–36768842	378	9.892	42.02
GmLPAT3	Glyma.04G026500	Gm4 2142017–2148415	388	9.161	43.61
GmLPAT4	Glyma.06G026500	Gm6 2032806–2036004	248	8.382	28.06
GmLPAT5	Glyma.06G220300	Gm6 25070446–25081599	348	10.097	38.50
GmLPAT6	Glyma.10G095500	Gm10 13758064–13771475	384	9.637	43.18
GmLPAT7	Glyma.11G120600	Gm11 9176591–9180658	376	8.818	43.26
GmLPAT8	Glyma.12G045700	Gm12 3302152–3306082	376	9.214	43.24
GmLPAT9	Glyma.12G163500	Gm12 33116752–33122217	356	10.231	39.58
GmLPAT10	Glyma.14G077500	Gm14 6425125–6429260	384	9.062	44.11
GmLPAT11	Glyma.14G216800	Gm14 49011220–49014983	397	8.302	44.73
GmLPAT12	Glyma.15G034100	Gm15 2715118–2721322	457	5.127	50.50
GmLPAT13	Glyma.17G248200	Gm17 40451620–40456023	384	9.025	44.06
GmLPAT14	Glyma.17G255400	Gm17 41041415–41044732	387	8.039	43.41
GmLPAT15	Glyma.19G142500	Gm19 40791453–40802147	388	9.796	43.27

[1)] IDs are available in the Phytozome database (https://phytozome-next.jgi.doe.gov/).

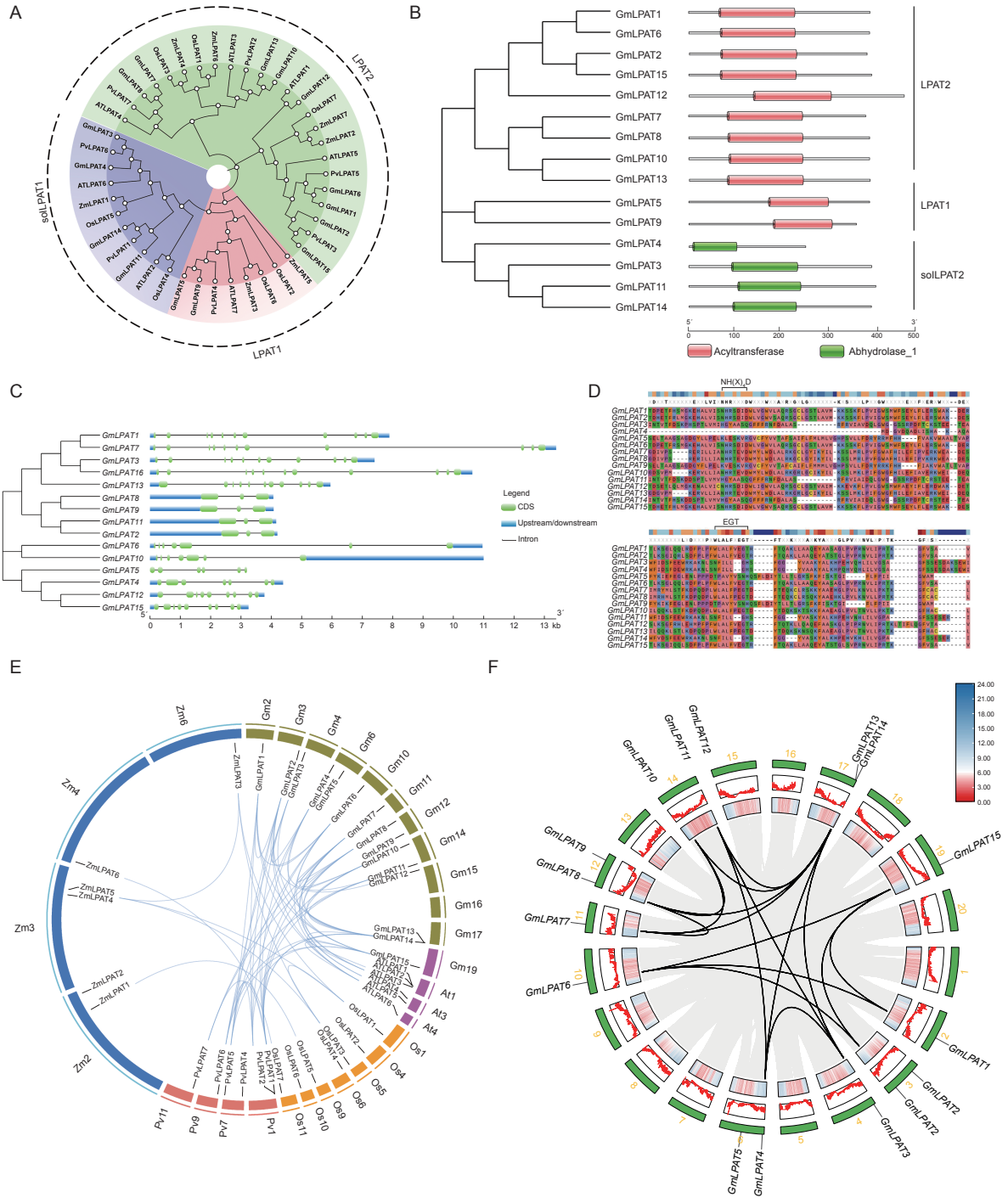

Fig. 1 Phylogenetic analysis, protein domain and collinearity analysis of the lysophosphatidic acid acyltransferase (LPAT) gene family. A, evolutionary analyses of the LPATs encoded by *Glycine max* (L.) Merr., *Arabidopsis thaliana* (L.) Heynh., *Phaseolus vulgaris* L., *Zea mays* L., and *Oryza sativa* L. B, the LPAT protein domain. C, *GmLPAT* exon-intron structures. D, GmLPAT protein sequence alignment results. E, synteny analyses of the LPAT genes encoded by *Z. mays*, *P. vulgaris*, *A. thaliana*, *G. max*, and *O. sativa*. F, synteny analyses of *GmLPAT* genes. Circles represent chromosomes, while differently colored curves denote syntenic *LPAT* gene areas.

common bean genomes were compared to gain further insight into *GmLPAT* evolution (Fig. 1-E). These *GmLPAT*s were distributed across 11 of the 20 soybean chromosomes, with multiple genes on chromosomes 3, 6, 12, 14, and 17, while one gene was present on each of the remaining six chromosomes (Appendix C). A total of 50 homologous *LPAT* gene pairs were identified among the five species, including 10 pairs between *Arabidopsis* and soybean, 21 between common bean and soybean (Fig. 1-F), one within rice, six between rice and maize, three within common bean, and one within maize. The soybean genome harbored 18 homologous gene pairs, primarily among related subfamilies. These syntenic events suggest that many of the identified *LPAT* genes evolved before the divergence of soybean species.

3.3. *cis*-Acting regulatory element analyses of *GmLPAT* promoters

The putative *cis*-acting regulatory elements within the promoters upstream of each of these *GmLPATs* were identified using predictive analysis (Fig. 2). Most of the *GmLPAT* promoters contain hormone-responsive elements, including abscisic acid response elements (ABREs) and methyl jasmonate (MeJA) response elements (TGACG, CGTCA). Elements responsive to specific stressors were also identified, including low-temperature response (LTR) elements and light-responsive elements, such as AE-BOX, G-BOX, and GATA motifs. These findings suggest roles for *GmLPATs* in plant development and stress response regulation.

3.4. Subcellular localization and enzyme kinetic analyses

GFP-tagged versions of six *GmLPATs* were transiently expressed in *Arabidopsis* mesophyll protoplasts, with 35S:GFP as a positive control. Of these, GmLPAT6, GmLPAT9, and GmLPAT10 were localized to the endoplasmic reticulum (Fig. 3-A), while GFP-tagged GmLPAT3, GmLPAT5, and GmLPAT11 were detected only in chloroplasts, indicating chloroplast localization (Fig. 3-B). These results align with online predictive analyses, offering new insight into plant LPAT localization at the subcellular level.

The potential role of *GmLPAT11* in stress resistance was explored preliminarily. A His-tagged *GmLPAT11* plasmid was expressed in *E. coli* for crude protein purification. SDS-PAGE analyses were used to assess the molecular weight of GmLPAT11-His (Fig. 4-C), while kinetic studies of the enzymatic activity of recombinant GmLPAT11 were performed with C18:1 LPA as the substrate. The Eadie-Hofstee plot was used to establish the kinetic parameters for this enzyme with C18:1

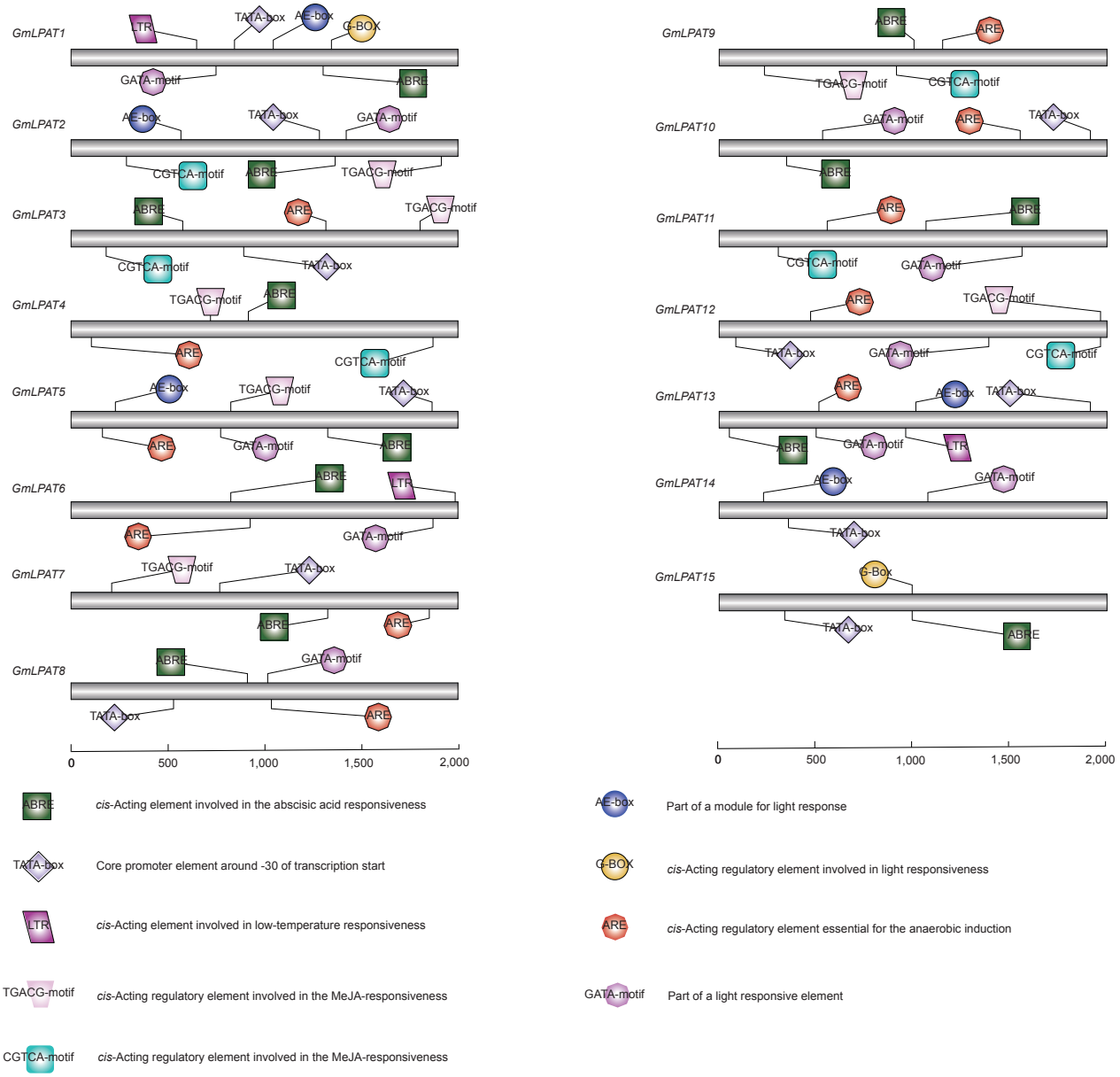

Fig. 2 *cis*-Acting regulatory element predictive analyses of *GmLPAT* promoter regions. Different colors of the boxes provide an approximation of the relative positions of these *cis*-acting elements upstream of each *GmLPAT*. MeJA, methyl jasmonate.

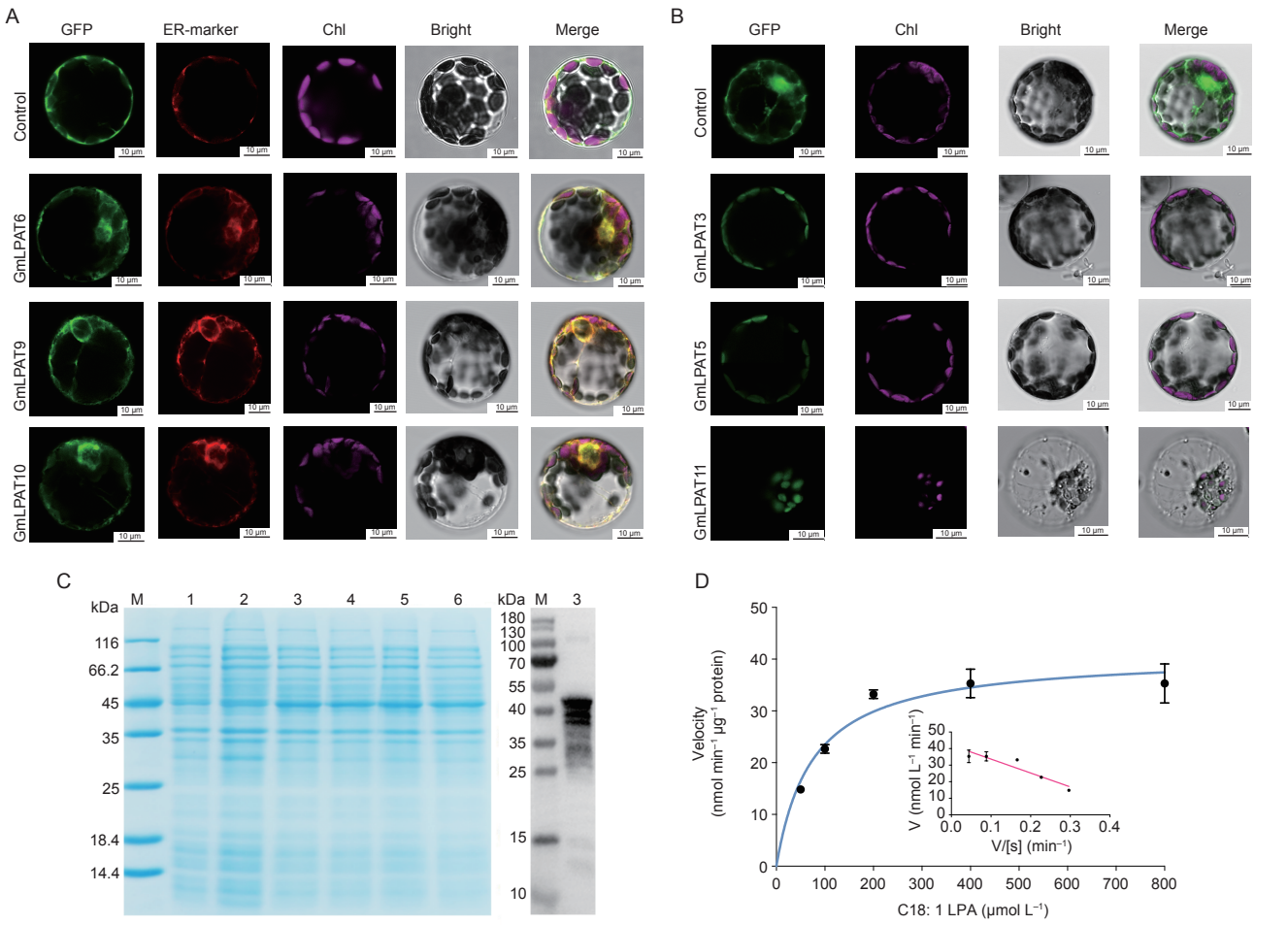

Fig. 3 GmLPAT subcellular localization analysis. A, subcellular localization of GmLPAT6, 8, 9, and 10 by confocal imaging in *Arabidopsis thaliana* mesophyll protoplasts transiently transfected with six GmLPAT-GFP fusion proteins. B, subcellular localization of GmLPAT3, 5, and 11. Scale bar=10 μm. C, SDS-PAGE and Western blotting analyses of purified recombinant GmLPAT11. D, Eadie-Hofstee plots generated for GmLPAT11 enzymatic reactions using C18:1 lysophosphatidic acid (LPA) as the substrate. V/[s], velocity/concentration of substrate. Bars mean SD (n=3).

LPA as a substrate, yielding a K_m of 74.14 nmol L^{-1} and V_{max} of 40.92 nmol min^{-1} μg^{-1} protein (Fig. 3-D). These results confirm the LPAT enzymatic activity of purified recombinant GmLPAT11.

3.5. Characterization of *GmLPAT* tissue expression patterns and responses to hormones or abiotic stressors

qPCR was used to assess the tissue-specific expression patterns of *GmLPATs* in soybean leaves, flowers, pods, seeds, stems, roots, nodules, and shoot apex samples. The *GmLPATs* were expressed in both reproductive and vegetative tissues (Yu *et al.* 2021). *GmLPAT11* was expressed at high levels in all analyzed tissue types compared to the other *GmLPATs*. Members of the *GmLPAT* family likely play distinct roles in soybean growth and development based on their tissue-specific expression patterns (Fig. 4-A). The transcriptional responses of these *GmLPATs* to salt (150 mmol L^{-1} NaCl), alkali (100 mmol L^{-1} $NaHCO_3$), and osmotic (20% PEG or 200 mmol L^{-1} mannitol) stress conditions were also analyzed. Under salt stress, *GmLPATs* were markedly upregulated, with *GmLPAT5* showing peak expression at 6 h post-treatment. After 3 h of alkaline treatment, *GmLPAT12* showed significantly increased expression compared to the other *GmLPATs*. Most *GmLPATs* were upregulated at later stages of alkaline stress, while some were downregulated. Osmotic stress did not significantly affect *GmLPAT* expression levels.

Plant hormones, including ABA, SA, BR, and MeJA, can influence stress signaling in plants (Wang *et al.* 2016). To clarify the responses of *GmLPAT* transcription to phytohormone stimulation, the mRNA levels of these 15 *GmLPATs* were analyzed in response to SA, JA, BR, and ABA treatments. Most *GmLPATs* were rapidly upregulated in response to JA treatment and stayed elevated throughout the experimental period. Most *GmLPATs* showed increased expression 6 h after BR treatment, while *GmLPAT1*, *GmLPAT2*, *GmLPAT7*, *GmLPAT8*, and *GmLPAT15* exhibited temporary upregulation at this time. SA or ABA treatment failed to significantly alter *GmLPAT* expression. Overall, most *GmLPATs* are associated with plant responses to JA and BR treatment (Fig. 5-B).

3.6. Overexpressing *GmLPAT11* enhances soybean salt tolerance

Soybean hairy roots overexpressing *GmLPAT11* were

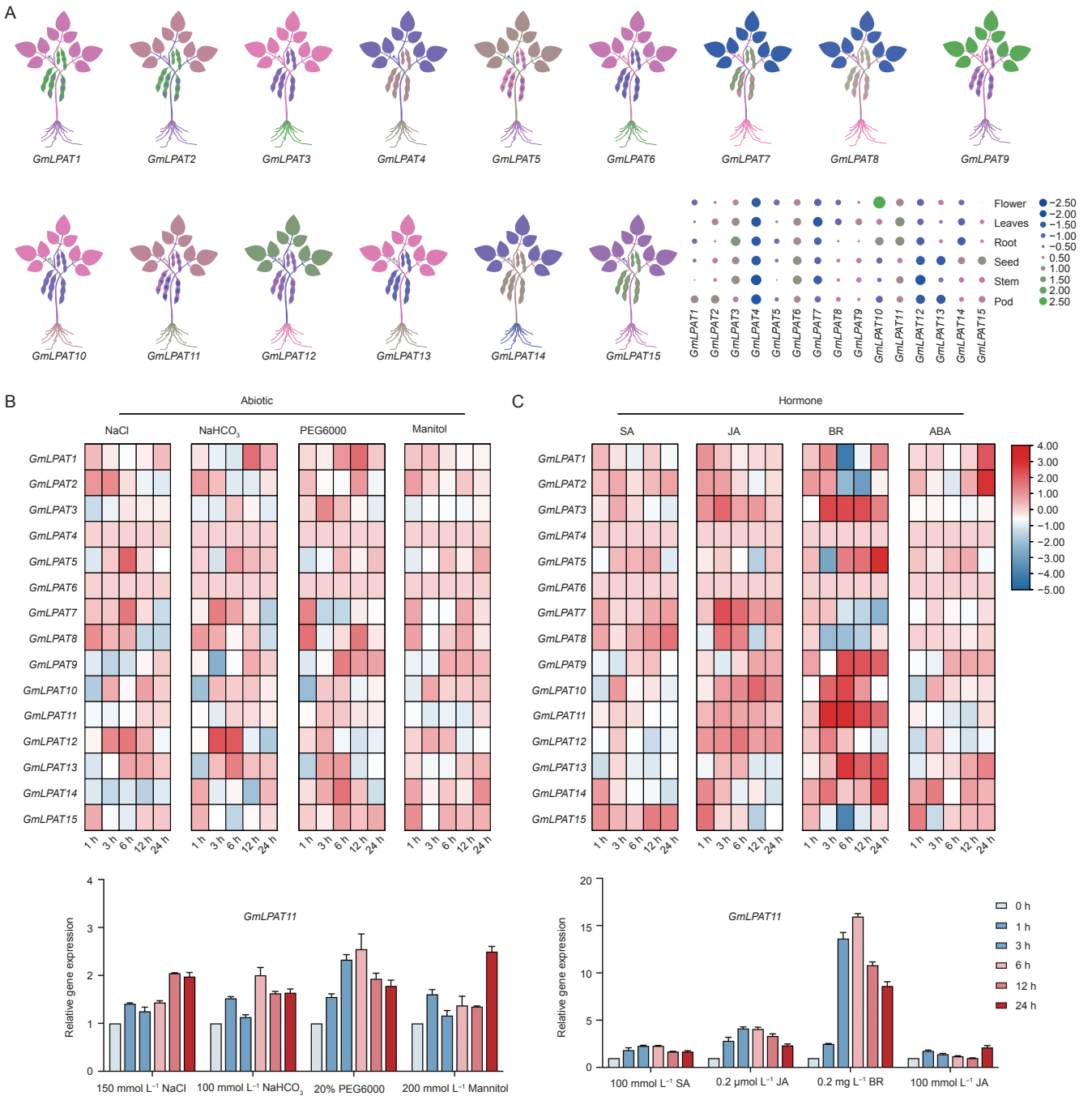

Fig. 4 Expression levels of *GmLPAT* genes in soybean plants and their expression levels under non-biological stress and hormone treatments. A, tissue-specific *GmLPAT* expression profiling. The $\log_2$ expression levels were used to generate a heatmap in Tbtools, with green and blue corresponding to low and high levels of transcription, respectively. B, GmLPAT expression levels following treatment with the indicated abiotic stressors or water (as a negative control) for 0, 1, 3, 6, 12, and 24 h. C, GmLPAT transcriptional profiles in soybean roots subjected to treatment with water (as a negative control), 100 μmol L^{-1} abscisic acid (ABA), salicylic acid (SA), brassinosteroids (BR), or jasmonic acid (JA) for 0, 1, 3, 6, 12, or 24 h. Bars mean SD (n=3). *, P<0.05; **, P<0.01; Student's t-test.

generated to examine the effects of *GmLPAT11* on plant responses to high salinity. *GmLPAT11* mRNA levels were elevated in overexpressing (OE1–OE12) compared to wild-type (WT) hairy roots (Appendix D). The LPAT enzymatic activities in OE lines were 2.8- to 5.0-fold higher than in WT hairy roots (Appendix D), confirming *GmLPAT11* overexpression. The two lines with the highest levels of *GmLPAT11* expression (OE1 and OE2) were chosen for further research. Overexpressing *GmLPAT11* failed to impact the growth of these soybean plants under normal conditions, with no apparent differences between the WT and OE plants (Fig. 5-A). However, differences between the two were apparent following salt treatment. Specifically, on day 3 of NaCl treatment, *GmLPAT11* overexpression was associated with root length, plant height, dry weight, and fresh weight

values that were all larger than those of WT plants, confirming the ability of *GmLPAT11* overexpression to enhance saline-alkali stress tolerance in soybean plants (Fig. 5-C).

3.7. *GmLPAT11* shapes cellular redox status and reactive oxygen species (ROS) homeostasis under salt stress

Propidium iodide (PI), which cannot penetrate intact cell membranes, was used to identify dead or damaged cells. PI staining of the root tips of different soybean lines was performed after 12 h of NaCl treatment. Under basal conditions, PI staining was minimal in the WT, OE1, and OE2 lines, with no differences among them. After 120 mmol L^{-1} NaCl treatment, all lines showed increased PI staining intensity, indicating some level of membrane damage and cell death. Compared to WT plants, the OE1 and OE2 lines showed reduced PI staining (Fig. 6-B), suggesting that *GmLPAT11* overexpression reduces membrane damage and cell death under salt stress.

The CoroNa™ Green sodium ion indicator, which emits a strong green fluorescent signal following Na^+ binding, was then used to stain soybean roots after NaCl treatment for 12 h. Under basal conditions, minimal CoroNa staining was evident for the WT, OE1, and OE2 lines, with no significant differences among these lines. However, after 120 mmol L^{-1} NaCl treatment, all lines showed increased staining intensity consistent with stress-induced Na^+ accumulation (Fig. 6-B). The OE1 and OE2 lines showed reduced CoroNa staining compared to WT plants, suggesting that *GmLPAT11* overexpression enhances salt tolerance by promoting root Na^+ ion efflux.

The H_2O_2 and $O_2^{-}\cdot$ levels were also analyzed in these soybean lines to further confirm the above results. Both H_2O_2 and $O_2^{-}\cdot$ levels were low and similar among the WT, OE1, and OE2 lines under basal conditions. However, NaCl stress increased H_2O_2 and $O_2^{-}\cdot$ levels in the roots of all analyzed lines, with significantly higher levels in samples from WT plants relative to the OE1 and OE2 lines. Therefore, *GmLPAT11* overexpression can limit salt stress-associated ROS accumulation to protect these plants against oxidative injury.

Considering the lower ROS levels observed in soybean plants overexpressing *GmLPAT11* after exposure to salt stress, the potential link between reduced ROS levels and enhanced antioxidant activity was evaluated. These analyses focused on the activity levels of superoxide dismutase (SOD; converts $O_2^{-}\cdot$ to H_2O_2 and O_2), catalase (CAT; converts H_2O_2 to H_2O and O_2), and ascorbate peroxidase (APX; converts H_2O_2 to H_2O and O_2). In the absence of stress, the SOD, CAT, and APX activity levels were similar among all lines. However, the SOD, CAT, and APX activity levels in the OE1 and OE2 lines after NaCl stress were higher than those for WT plants (Fig. 6-C). This indicates that *GmLPAT11* overexpression can strengthen the antioxidant capacity of soybean plants.

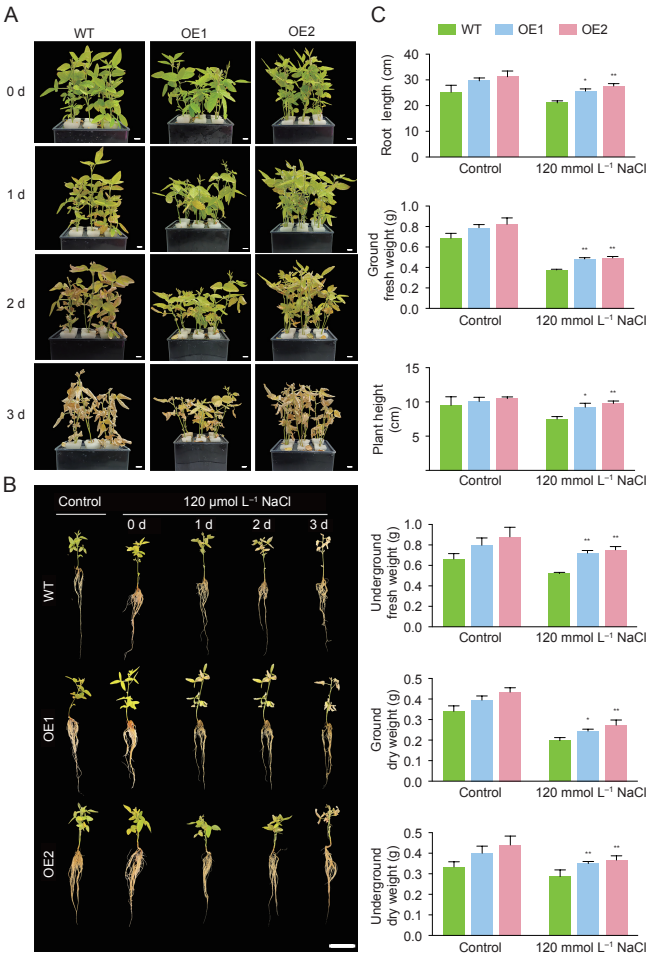

Fig. 5 *GmLPAT11* overexpression enhances the salt tolerance of transgenic soybean hairy roots. A and B, plant performance under the indicated conditions. Scale bar=1 cm. C, control and *GmLPAT11*-overexpressing soybean hairy root parameters following treatment for 3 d with 120 mmol L^{-1} NaCl. Bars mean SD (n=3). *, P<0.05; **, P<0.01; Student's t-test.

3.8. Haplotype analyses of *GmLPAT11*

Genome-wide sequencing and candidate gene association analyses have been widely used in crop species to identify beneficial alleles. This approach narrows the range of potential alleles and improves gene characterization accuracy, making it a valuable tool for evaluating candidate genes. For haplotype screening and the determination of major haplotypes, we referred to previous studies. Among the 547 germplasm resources in this study, we identified 23 haplotypes, with 383 and 75 soybean varieties belonging to Hap1 and Hap2, respectively, which are considered the major haplotypes. In total, 20 significant SNPs related to salt tolerance (P<0.01) were identified in the *GmLPAT11* gene based on analyses performed at the seedling stage, indicating a link between natural variation and the salt tolerant phenotypes. The natural *GmLPAT11* variation observed in this haplotype analysis may contribute to salt tolerance in soybean seedlings. However, further studies are needed to confirm whether the identified promoter polymorphisms affect gene expression and salt tolerance.

4. Discussion

4.1. Molecular characterization of the *GmLPAT* family

Comparative analyses of different species of plants have

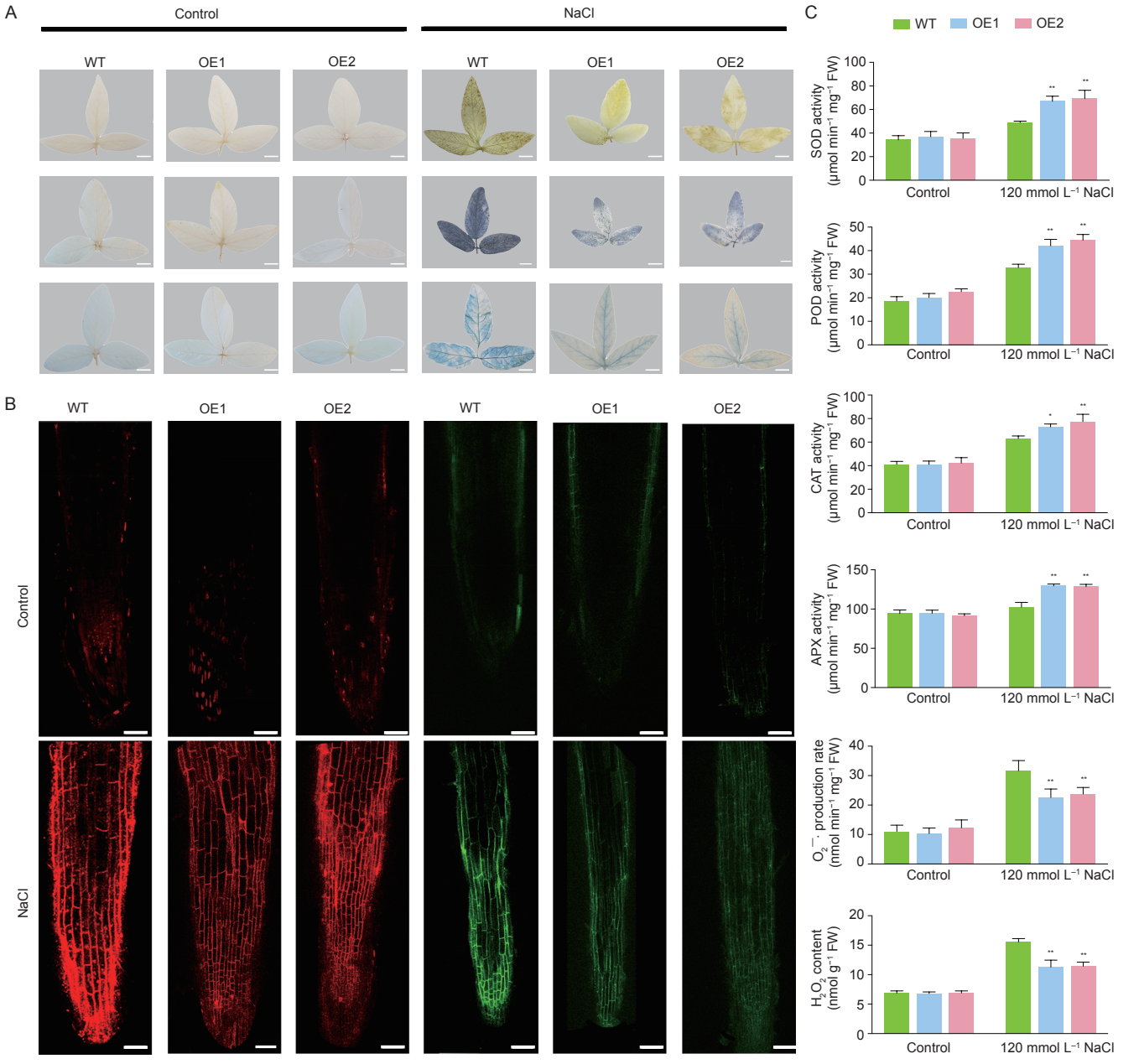

Fig. 6 *GmLPAT11* enhances soybean salt tolerance by regulating antioxidant activity and the oxidation-reduction state. A, nitrotetrazolium blue chloride (NBT), diaminobenzidine, 3,3′-diaminobenzidine (DAB), and Evans blue staining approaches were respectively used to detect superoxide ($O_2^{-}\cdot$), hydrogen peroxide (H_2O_2), and cell death levels under salt stress conditions. B, propidium Iodide (PI) staining-based detection of membrane injury in soybean lines subjected to salt stress, and CoroNa™ Green staining-mediated detection of Na^+ accumulation. Scale bar=50 μm. C, activities of ascorbate peroxidase (APX), peroxidase (POD), and catalase (CAT), $O_2^{-}\cdot$ and H_2O_2 levels in the roots of wild type (WT) and *GmLPAT11*-overexpressing plants treated for 3 d with NaCl (0 or 120 mmol L^{-1}). Bars mean SD (n=3). *, P<0.05; **, P<0.01 *vs*. WT; Student's *t*-test.

indicated the extensive expansion of the *LPAT* gene family throughout evolution (Misra *et al.* 2014). The phylogenetic analyses in this study demonstrated that *GmLPATs* and homologous genes in leguminous plants are closely related, reflecting functional conservation (Fig. 1-A). Collinearity observed between *GmLPATs* and the *LPATs* expressed by common bean and *Arabidopsis* plants indicates the potential emergence of *GmLPATs* before these species diverged (Fig. 1-E). Previous studies of the LPAT1, LPAT2, and solLPAT1 subtypes reported similar findings for subcellular localization, protein structure, and phylogeny, which were confirmed in this study (Misra *et al.* 2014). The LPATs within each subgroup showed similar intron-exon lengths and distributions. GFP-fused *GmLPAT3*, *GmLPAT4*, *GmLPAT5*, *GmLPAT6*, *GmLPAT9*, *GmLPAT10*, and *GmLPAT11* were expressed, with *GmLPAT4*, *GmLPAT6*, *GmLPAT9*, and *GmLPAT10* localizing to the endoplasmic reticulum, while *GmLPAT3*, *GmLPAT5*, and *GmLPAT11* were localized to chloroplasts. Different subtypes of GmLPATs thus appear to function in specific organelles. These results can

provide valuable insight into the functions of these different plant *LPAT* family members. *LPAT*s play key roles in lipid biosynthesis and stress response regulation in *Arabidopsis* (Kim *et al.* 2005), rice (Shaikh *et al.* 2022), maize (Brown *et al.* 1994; Chen *et al.* 2012), *B. napus* (Bourgis *et al.* 1999), castor bean (Arroyo-Caro *et al.* 2013), and tomato (Taylor *et al.* 2010) plants. In this study, qPCR showed *GmLPAT* expression in both reproductive and vegetative tissues of soybeans, suggesting roles in physiological processes essential for growth and development. *GmLPATs* were also significantly upregulated in response to hormone treatments and stressors, especially salt stress (Fig. 4). Promoter *cis*-acting regulatory elements likely mediate *GmLPAT* expression in response to abiotic stressors (Fig. 2), including hormone-responsive elements (ABRE, TGACG, and CGTCA), stress-responsive elements (LTR), and light-responsive motifs (AE-BOX, G-BOX, and GATA-motif). Enzymatic analyses of recombinant GmLPAT11 showed a substrate affinity (K_m) of 74.14 nmol L^{-1} (Fig. 3), consistent with the kinetic parameters described for other LPATs (Arroyo-Caro *et al.* 2013).

4.2. *GmLPAT11* enhances salt tolerance in soybean by regulating antioxidant activity and redox status

GmLPAT11 overexpression in soybean hairy roots resulted in significantly longer roots and higher root fresh weight than in WT plants under salt stress, indicating enhanced salt tolerance (Fig. 5), as was also reported in rice (Shaikh *et al.* 2022). PA is a key second messenger involved in the development of plants and the coordination of stress responses (Wang *et al.* 2024). In *Arabidopsis*, for instance, PA is important for responses to heat, cold, and drought conditions (Ruelland *et al.* 2015; Pokotylo *et al.* 2018). Abiotic stressors can disrupt redox homeostasis, leading to increased lipid peroxidation and oxidative stress, making redox balance essential for resistance (Hossain and Dietz 2016). Salt stress increased the APX, POD, and SOD activity levels in all soybean lines, with even higher levels observed in *GmLPAT11*-overexpressing plants than in WT controls. Cellular damage and the levels of H_2O_2 and $O_2^{-}\cdot$ were also analyzed, with *GmLPAT11*-overexpressing plants exhibiting reduced staining intensity in all three cases, consistent with reduced ROS accumulation and less severe cellular damage. The PI staining of root tips showed reduced intensity and fewer stained areas in *GmLPAT11*-overexpressing plants, indicating reduced membrane damage and cell death, thereby contributing to salt stress resistance. Under saline–alkali stress conditions, high soil Na^+ concentrations can disrupt the ionic balance in plant cells, leading to membrane structural damage and reduced metabolic activity, resulting in ion toxicity (Hasegawa 2013). CoroNa™ Green staining of WT and *GmLPAT11*-overexpressing roots showed lighter staining in the latter, suggesting improved salt tolerance through enhanced Na^+ root efflux.

4.3. *GmLPAT11* gene variants are closely related to soybean seedling salt tolerance

Advanced whole-genome sequencing and candidate gene association analyses have improved the accurate identification of beneficial alleles in many crops. At the seedling stage, 20 *GmLPAT11* SNPs associated with salt tolerance were identified (P<0.01), indicating a close association between natural genetic variation and salt tolerance. The *GmLPAT11* variants identified through this haplotype analysis suggest that natural variation in soybean tolerance to salt stress is at least partially attributable to *GmLPAT11* variation (Fig. 7). Further molecular analyses are needed to determine whether promoter polymorphisms in *GmLPAT11* or other soybean genes are functionally linked to differences in gene expression and salt tolerance.

5. Conclusion

This study identified 15 *LPAT* genes in the soybean genome. The products of these genes were classified into the LPAT1, LPAT2, and solLPAT1 subtypes through phylogenetic analyses. The observed differences in the expression patterns of specific *GmLPATs* under abiotic stress conditions suggest that they have different functions. The transcriptional response of *GmLPAT11* to salt stress indicates its potential role in coordinating soybean responses to abiotic stress. The mechanistic studies conducted in this study support a model wherein *GmLPAT11* can enhance soybean tolerance for saline-alkali stress by enhancing antioxidant activity and mitigating ROS accumulation. Together, these findings provide a basis for characterizing the functional roles of GmLPATs and other plant LPAT families in future studies.

Acknowledgements

This study was financially supported by the Natural Science Foundation of Heilongjiang Province, China (TD2022C003 and YQ2022C010), the National Key R&D Program of China (2023ZD040360305), and the National Natural Science Foundation of China (U20A2027, U23A201783, 32272093, and 32272072).

Declaration of competing interest

The authors declare that they have no conflict of interest.

Declaration of generative AI and AI-assisted technologies in the writing process

The authors declare that they did not use AI in the preparation and writing of this manuscript.

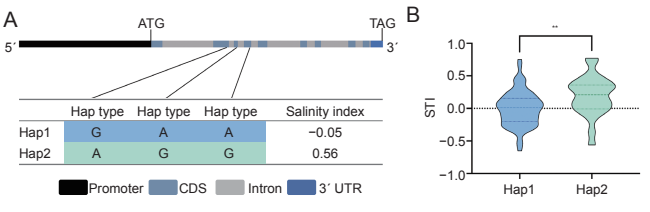

Fig. 7 Association and haplotype analyses of *GmLPAT11* in the context of salt tolerance in soybean plants. A, haplotype analysis of *GmLPAT11* from 547 soybean resources, with significant SNP locations indicated within the *GmLPAT11* gene structure. CDS, coding sequence. B, stress tolerance index (STI) comparisons for *GmLPAT11* haplotypes. **, P<0.01.

Appendices associated with this paper are available at https://doi.org/10.1016/j.jia.2024.12.031

References

Ali U, Lu S, Fadlalla T, Iqbal S, Yue H, Yang B, Hong Y, Wang X, Guo L. 2022. The functions of phospholipases and their hydrolysis products in plant growth, development and stress responses. *Progress in Lipid Research*, **86**, 101158.

Angkawijaya A E, Nguyen V C, Nakamura Y. 2017. Enhanced root growth in phosphate-starved *Arabidopsis* by stimulating *de novo* phospholipid biosynthesis through the overexpression of *LYSOPHOSPHATIDIC ACID ACYLTRANSFERASE 2* (*LPAT2*). *Plant Cell and Environment*, **40**, 1807–1818.

Arroyo-Caro J M, Chileh T, Kazachkov M, Zou J, Alonso D L, García-Maroto F. 2013. The multigene family of lysophosphatidate acyltransferase (LPAT)-related enzymes in *Ricinus communis*: Cloning and molecular characterization of two LPAT genes that are expressed in castor seeds. *Plant Science*, **199–200**, 29–40.

Bargmann B O R, Laxalt A M, Riet B T, van Schooten B, Merquiol E, Testerink C, Haring M A, Bartels D, Munnik T. 2008. Multiple PLDs required for high salinity and water deficit tolerance in plants. *Plant and Cell Physiology*, **50**, 78–89.

Bourgis F, Kader J C, Barret P, Renard M, Robinson D, Robinson C, Delseny M, Roscoe T J. 1999. A plastidial lysophosphatidic acid acyltransferase from oilseed rape. *Plant Physiology*, **120**, 913–922.

Brown A P, Coleman J, Tommey A M, Watson M D, Slabas A R. 1994. Isolation and characterisation of a maize cDNA that complements a 1-acyl sn-glycerol-3-phosphate acyltransferase mutant of *Escherichia coli* and encodes a protein which has similarities to other acyltransferases. *Plant Molecular Biology*, **26**, 211–223.

Bustin S A, Benes V, Garson J A, Hellemans J, Huggett J, Kubista M, Mueller R, Nolan T, Pfaffl M W, Shipley G L, Vandesompele J, Wittwer C T. 2009. The MIQE guidelines: Minimum information for publication of quantitative real-time PCR experiments. *Clinical Chemistry*, **55**, 611–622.

Chapman K D, Ohlrogge J B. 2012. Compartmentation of triacylglycerol accumulation in plants. *Journal of Biological Chemistry,* **287**, 2288–2294.

Chen J, Zhang P, Zhao Y, Zhao J, Wu X, Zhang R, Cha R, Yao Q, Gao Y. 2022. Nitroreductase-instructed supramolecular assemblies for microbiome regulation to enhance colorectal cancer treatments. *Science Advances*, **8**, eadd2789.

Chen S L, Huang J Q, Lei Y, Zhang Y T, Ren X P, Chen Y N, Jiang H F, Yan L Y, Li Y R, Liao B S. 2012. Identification and characterization of a gene encoding a putative lysophosphatidyl acyltransferase from *Arachis hypogaea*. *Journal of Bioscience and Bioengineering*, **37**, 1029–1039.

Chen X, Wang Y, Wang J N, Cao Q C, Sun R X, Zhu H J, Zhang Y R, Ji J D, Liu Q H. 2022. m^{6}A modification of circSPECC1 suppresses RPE oxidative damage and maintains retinal homeostasis. *Cell Reports*, **41**, 111671.

Chen Y, Fu Z, Zhang H, Tian R, Yang H, Sun C, Wang L, Zhang W, Guo Z, Zhang X, Tang J. 2020. Cytosolic malate dehydrogenase 4 modulates cellular energetics and storage reserve accumulation in maize endosperm. *Plant Biotechnology Journal*, **18**, 2420–2435.

Dai H F Wu H, Amanguli Maimaiti Ali A, Wang L H, Apizi M, Zhang J S. 2014. Analysis of salt-tolerance and determination of salt-tolerant evaluation indicators in cotton seedlings of different genotypes. *Scientia Agricultura Sinica*, **47**, 1290–1300. (in Chinese)

Fryer M J, Oxborough K, Mullineaux P M, Baker N R. 2002. Imaging of photo-oxidative stress responses in leaves. *Journal of Experimental Botany*, **53**, 1249–1254.

Giannopolitis C N, Ries S K. 1977. Superoxide dismutases: I. Occurrence in higher plants. *Plant Physiology*, **59**, 309–314.

Han R H, Lu X S, Gao G J, Yang X J. 2006. Analysis of the principal components and the subordinate function of alfalfa drought resistance. *Acta Agrestia Sinica*, **14**, 142–146. (in Chinese)

Hanke C, Wolter F P, Coleman J, Peterek G, Frentzen M. 1995. A plant acyltransferase involved in triacylglycerol biosynthesis complements an *Escherichia coli* sn-1-acylglycerol-3-phosphate acyltransferase mutant. *European Journal of Biochemistry*, **232**, 806–810.

Hasegawa P M. 2013. Sodium (Na^+) homeostasis and salt tolerance of plants. *Environmental and Experimental Botany*, **92**, 19–31.

Hong Y, Pan X, Welti R, Wang X. 2008. Phospholipase Dα3 is involved in the hyperosmotic response in *Arabidopsis*. *The Plant Cell*, **20**, 803–816.

Hong Y, Zhao J, Guo L, Kim S C, Deng X, Wang G, Zhang G, Li M, Wang X. 2016. Plant phospholipases D and C and their diverse functions in stress responses. *Progress in Lipid Research*, **62**, 55–74.

Hossain M S, Dietz K J. 2016. Tuning of redox regulatory mechanisms, reactive oxygen species and redox homeostasis under salinity stress. *Frontiers in Plant Science*, **7**, 548.

Kim H U, Huang A H C. 2004. Plastid lysophosphatidyl acyltransferase is essential for embryo development in *Arabidopsis*. *Plant Physiology*, **134**, 1206–1216.

Kim H U, Li Y, Huang A H. 2005. Ubiquitous and endoplasmic reticulum-located lysophosphatidyl acyltransferase, LPAT2, is essential for female but not male gametophyte development in *Arabidopsis*. *Plant Cell*, **17**, 1073–1089.

Kim H U, Vijayan P, Carlsson A S, Barkan L, Browse J. 2010. A mutation in the *LPAT1* gene suppresses the sensitivity of *fab1* plants to low temperature. *Plant Physiology*, **153**, 1135–1143.

Knutzon D S, Lardizabal K D, Nelsen J S, Bleibaum J L, Davies H M, Metz J G. 1995. Cloning of a coconut endosperm cDNA encoding a 1-acyl-sn-glycerol-3-phosphate acyltransferase that accepts medium-chain-length substrates. *Plant Physiology*, **109**, 999–1006.

Kolkman J A, Stemmer W P. 2001. Directed evolution of proteins by exon shuffling. *Nature Biotechnology*, **19**, 423–428.

Lewin T M, Wang P, Coleman R A. 1999. Analysis of amino acid motifs diagnostic for the sn-glycerol-3-phosphate acyltransferase reaction. *Biochemistry*, **38**, 5764–5771.

Liu M, Wu S, Walch H, Grigoriev A. 2005. Exon-domain correlation and its corollaries. *Bioinformatics*, **21**, 3213–3216.

Liu W, Xie Y, Ma J, Luo X, Nie P, Zuo Z, Lahrmann U, Zhao Q, Zheng Y, Zhao Y, Xue Y, Ren J. 2015. IBS: An illustrator for the presentation and visualization of biological sequences. *Bioinformatics*, **31**, 3359–3361.

Maisonneuve S, Bessoule J J, Lessire R, Delseny M, Roscoe T J. 2010. Expression of rapeseed microsomal lysophosphatidic acid acyltransferase isozymes enhances seed oil content in *Arabidopsis*. *Plant Physiology*, **152**, 670–684.

Mishra G, Zhang W, Deng F, Zhao J, Wang X. 2006. A bifurcating pathway directs abscisic acid effects on stomatal closure and opening in *Arabidopsis*. *Science*, **312**, 264–266.

Misra N, Panda P K, Parida B K. 2014. Genome-wide identification and evolutionary analysis of algal LPAT genes involved in TAG biosynthesis using bioinformatic approaches. *Molecular Biology Reports*, **41**, 8319–8332.

Nakano Y, Asada K. 1981. Hydrogen peroxide is scavenged by ascorbate-specific peroxidase in spinach chloroplasts. *Plant and Cell Physiology*, **22**, 867–880.

Ohlrogge J, Browse J. 1995. Lipid biosynthesis. *The Plant Cell*, **7**, 957–970.

Pokotylo I, Kravets V, Martinec J, Ruelland E. 2018. The phosphatidic acid paradox: Too many actions for one molecule class? Lessons from plants. *Progress in Lipid Research*, **71**, 43–53.

Ruelland E, Kravets V, Derevyanchuk M, Martinec J, Zachowski A, Pokotylo I. 2015. Role of phospholipid signalling in plant environmental responses. *Environmental and Experimental Botany*, **114**, 129–143.

Shaikh A A, Alamin A, Jia C, Gong W, Deng X, Shen Q, Hong Y. 2022. The examination of the role of rice lysophosphatidic acid acyltransferase 2 in response to salt and drought stresses. *International Journal of Molecular Sciences*, **23**, 9796.

Sivakumar D, Sivaraman T. 2011. *In silico* designing and screening of lead compounds to NS5-methyltransferase of dengue viruses. *Journal of Medicinal Chemistry*, **7**, 655–662.

Snyder C L, Yurchenko O P, Siloto R M, Chen X, Liu Q, Mietkiewska E, Weselake R J. 2009. Acyltransferase action in the modification of seed oil biosynthesis. *Nature Biotechnology*, **26**, 11–16.

Tambasco-Studart M, Titiz O, Raschle T, Forster G, Amrhein N, Fitzpatrick T B. 2005. Vitamin B6 biosynthesis in higher plants. *Proceedings of the National Academy of Sciences of the United States of America*, **102**, 13687–13692.

Taylor D C, Francis T, Lozinsky S, Hoffman T L, Giblin M E, Marillia E F.

2010. Cloning and characterization of a constitutive lysophosphatidic acid acyltransferase 2 (*LPAT2*) gene from *Tropaeolum majus* L. *The Open Plant Science Journal*, **4**, 7–17.

Tóth K, Batek J, Stacey G. 2016. Generation of soybean (*Glycine max*) transient transgenic roots. *Current Protocols in Plant Biology*, **1**, 1–13.

Velikova V, Yordanov I, Edreva A. 2000. Oxidative stress and some antioxidant systems in acid rain-treated bean plants: Protective role of exogenous polyamines. *Plant Science*, **151**, 59–66.

Wang D, Yuan M, Zhuang Y, Xin X F, Qi G. 2024. DGK5-mediated phosphatidic acid homeostasis interplays with reactive oxygen species in plant immune signaling. *Journal of Integrative Plant Biology*, **66**, 1263–1265.

Wang P, Shen L, Guo J, Jing W, Qu Y, Li W, Bi R, Xuan W, Zhang Q, Zhang W. 2019. Phosphatidic acid directly regulates PINOID-dependent phosphorylation and activation of the PIN-FORMED2 auxin efflux transporter in response to salt stress. *The Plant Cell*, **31**, 250–271.

Wang Q J, Sun H, Dong Q L, Sun T Y, Jin Z X, Hao Y J, Yao Y X. 2016. The enhancement of tolerance to salt and cold stresses by modifying the redox state and salicylic acid content *via* the cytosolic malate dehydrogenase gene in transgenic apple plants. *Plant Biotechnology Journal*, **14**, 1986–1997.

Wang X, Devaiah S P, Zhang W, Welti R. 2006. Signaling functions of phosphatidic acid. *Progress in Lipid Research*, **45**, 250–278.

Yoo S D, Cho Y H, Sheen J. 2007. *Arabidopsis* mesophyll protoplasts: A versatile cell system for transient gene expression analysis. *Nature Protocols*, **2**, 1565–1572.

Yu C Y, Zhang H K, Wang N, Sun J, Dong Y X, Zhang X S, Gao X Q. 2021. Characterization of the ERP gene family in *Arabidopsis thaliana*. *Plant Signaling and Behavior*, **16**, 1913301.

Zhang Q, Lin F, Mao T, Nie J, Yan M, Yuan M, Zhang W. 2012. Phosphatidic acid regulates microtubule organization by interacting with MAP65-1 in response to salt stress in *Arabidopsis*. *The Plant Cell*, **24**, 4555–4576.

Zhang R, Hussain S, Wang Y, Liu Y, Li Q, Chen Y, Wei H, Gao P, Dai Q. 2021. Comprehensive evaluation of salt tolerance in rice (*Oryza sativa* L.) germplasm at the germination stage. *Agronomy*, **11**, 1569.

Zhang W, Qin C, Zhao J, Wang X. 2004. Phospholipase Dα1-derived phosphatidic acid interacts with ABI1 phosphatase 2C and regulates abscisic acid signaling. *Proceedings of the National Academy of Sciences of the United States of America*, **101**, 9508–9513.

Zhao Y, Cao P, Cui Y, Liu D, Li J, Zhao Y, Yang S, Zhang B, Zhou R, Sun M, Guo X, Yang M, Xin D, Zhang Z, Li X, Lv C, Liu C, Qi Z, Xu J, Wu X, Chen Q. 2021. Enhanced production of seed oil with improved fatty acid composition by overexpressing NAD^+-dependent glycerol-3-phosphate dehydrogenase in soybean. *Journal of Integrative Plant Biology*, **63**, 1036–1053.

Zhou R N, Wang S H, Liu P Y, Cui Y F, Hu Z B, Liu C Y, Zhang Z G, Yang M L, Li X, Wu X X, Chen Q S, Zhao Y. 2025. Genome-wide characterization of soybean malate dehydrogenase genes reveals a positive role for *GmMDH2* in the salt stress response. *Journal of Integrative Agriculture*, **24**, 2492–2510.